Detection of Passive Liver Congestion in Pericarditis Patients With Constrictive Physiology Using MR Relaxometry of the Liver.

Jan Bogaert (jan.bogaert@uzleuven.be)
KU Leuven
Tom Dresselaers
KU Leuven
Massimo Imazio
Azienda Ospedaliera Citta' Della Salute E Della Scienza Di Torino
Peter Sinnaeve
KU Leuven
Luigi Tassetti
KU Leuven
Pier Giorgio Masci
King's College London
Rolf Symons
KU Leuven

Research Article

Keywords: Constrictive, pericarditis, liver, AUC

Posted Date: December 4th, 2020

DOI: https://doi.org/10.21203/rs.3.rs-114965/v1

Abstract

Constrictive pericarditis is a common cause of right heart failure, characterized by increased filling pressures and passive liver congestion. As magnetic resonance (MR) T1 and T2 mapping allow quantification of liver relaxation times, we hypothesized liver mapping may allow depiction of passive liver congestion. We studied 45 pericarditis patients, of whom 25 presented constrictive physiology (CP+) and 20 normal physiology (CP-), and 30 control subjects. Pericarditis patients were predominantly male, but CP+ patients were on average 13 years older than CP- patients (p=0.003). Native T1 and T2 values as well as extracellular volume (ECV) values of the liver were significantly higher in CP+ than in CP- patients and controls, i.e. native T1: 765±102ms vs 581±56ms and 537±30ms; T2: 63±13ms vs 50±4ms and 46±4ms; ECV: 42±7% vs 31±3% and 30±3% control (all p<0.001). Using a cut-off right atrial (RA) pressure of >5 mm Hg to discriminate between normal and increased RA pressure, native T1 liver yielded the highest AUC (0.926) at ROC analysis with a sensitivity of 79.3% and specificity of 95.6%. Moreover, liver mapping showed excellent intra- and inter-reader agreement. In conclusion, liver mapping as part of a comprehensive cardiovascular MR exam is valuable to depict liver congestion in pericarditis patients.

Introduction

Congestive heart failure in patients with constrictive pericardial physiology is caused by

increased right heart filling pressure leading to passive liver congestion induced by impaired hepatic venous outflow, a condition also called congestive hepatopathy [1,2]. Timely recognition of liver congestion is crucial as this condition may cause liver fibrosis and eventually cirrhosis. As the patients' symptoms and clinical findings in congestive hepatopathy vary and may appear only at later stages, early detection of this condition is challenging on clinical grounds only. A combination of right atrial (RA) pressure measurements at transthoracic echography (TTE) or cardiac catheterization coupled with liver markers of cholestasis are currently considered the mainstay feature of congestive hepatopathy [2,4,5]. Abnormal liver ultrasound or contrast-enhanced computed tomography may be used to confirm this condition [3]. Novel techniques, such as assessment of the elastic properties of the liver using magnetic resonance (MR) elastography, are appealing not only to study patients with primary liver diseases but also to study liver stiffness in patients with heart failure [6-8]. However, MR elastography is not yet integrated in routine clinical practice given the complex acquisition, time-consuming post-processing and the requirement of an additional vibration device [6].

Cardiovascular MR imaging allows to comprehensively assess the heterogeneous spectrum of patients with pericarditis, ranging from acute pericarditis to end-stage constrictive pericarditis [9,10]. It is important to emphasize that constrictive physiology may occur in any condition where the pericardial compliance is decreased, thus not only in healed, fibrotic stages of pericarditis but also in acute conditions with active or ongoing pericardial inflammation. A typical, almost pathognomonic, hallmark of constrictive pericardial physiology is an increased ventricular coupling, a phenomenon which can be studied using free-breathing real-time cine CMR [11]. In recent years, quantitative, parametric imaging of the heart, using

T1 and T2 MR relaxometry (the so-called mapping techniques), has become part of a standard CMR exam in ischemic and non-ischemic myocardial diseases [12]. Moreover, information with regard to the myocardial extracellular volume (ECV) can be obtained when T1 mapping is repeated post-contrast [12]. Clinical conditions with increased water content, such in patients with acute myocardial infarction, can be accurately depicted at T1 and T2 mapping [13].

In this monocentric, observational study, we hypothesized that in patients with pericardial disease MR mapping of the liver can complement cardiac imaging by unravelling co-existing congestive hepatopathy. To test this hypothesis, we determined native and post-contrast T1 and T2 values of the liver parenchyma, obtained during a routine cardiovascular MR imaging study, and correlated these findings to constrictive physiology pattern, RA pressures and other features of congestive hepatopathy.

Results

General patient data (Table 1)

CP+ and CP- patients were predominantly male, but CP+ patients were on average 13 years older than CP- patients (p=0.003). The majority of patients (75%) in the CP+ group had predisposing factors for developing constricting, i.e., history of pericarditis (n=17), cardiac surgery (n=2), radiation therapy (n=3), systemic inflammatory disease (n=2). Eleven patients underwent pericardiectomy while the others received optimized anti-inflammatory treatment. In the CP- group, nine patients had a history of previous/recurrent pericarditis, two patients had cardiac surgery. All CP- patients received anti-inflammatory therapy. Typical pericarditis-like chest pain was present in 9(36%) and 19(95%) of CP+ and CP- patients, respectively. CP+ patients had a higher heart rate than CP- patients (p<0.001). Dyspnea with NYHA class was present in 20 CP+ patients versus 3 CP- patients (p<0.001). Clinical examination showed raised central venous pressure in 13(52%) and lower limb edema in 9(36%) of CP+ patients, but in none of the CP- patients (both p<0.001). Atrial fibrillation was present in 6 CP+, 2 CP- patients and in none of the controls (p=0.004). Prior to CMR, pericardiocentesis was performed in 5 CP+ patients and 1 CP- patient.

Laboratory findings (Table 1)

CP+ patients had lower hematocrit values than controls (38.3±5.4 % *vs* 43.0±2.7 %; p<0.001). CRP values and troponin-I values were increased in both patient groups. Gamma-glutamyl transferase (GGT), alkaline phosphatase and total bilirubin values were higher in the CP+ compared to the CP- and control groups, (p<0.001, p<0.001 and p=0.006, respectively). Moreover, CP+ patients showed slightly but significantly higher aspartate transaminase (AST) values than controls (p=0.006).

Transthoracic echocardiography and right heart catheterization (Table 1)

Transthoracic echocardiography (TTE) showed a dilated inferior vena cava (IVC) in 17(68%) of CP+ patients versus 1(5%) of CP- patients (p<0.001). Respiratory variation of the IVC was absent in 20(80%)

of CP+ patients versus 1(5%) of CP- patients (p<0.001). RA pressure estimates were significantly higher in the CP+ than in the CP- group (p<0.001). At right heart catheterization, performed in 15 CP+ subjects, right atrial pressure was 20mm Hg (IQR:18-22mm Hg).

Cardiovascular MR imaging findings (Table 2)

CP+ patients had lower left ventricular (LV) and right ventricular (RV) end-diastolic volume (EDV) volumes (both p<0.001), and a lower RV ejection fraction (EF) (p=0.005) than CP- patients and controls. Whereas no differences in native T1 and T2 myocardial values were found, CP+ patients showed slight but significantly higher ECV myocardial values than CP- patients and controls (p=0.003). Pericardial thickness was higher in the CP+ group, i.e., 5mm (4-11mm), versus 1.7mm (1.3-3.4mm) and 1.1mm (1.0-1.3 mm) in the CP- and control group, respectively (p<0.001). A pericardial effusion was found in 11 CP+ patients (44%) vs in 4 CP- (20%) and in 5 control subjects (17%) (Fig 1). Pericardial edema (T2-hyperintense) was found in 4(16%) and 6(30%) CP+ and CP- patients, respectively. Pericardial inflammation (late gadolinium enhancement (LGE)-positive) was present in 23 (92%) and 20 (100%) CP+ and CP- patients, respectively. A pleural effusion was more often seen in CP+ patients (p<0.001). Atrial size was not different between groups. However, CP+ patients showed larger IVC resulting in a higher IVC/aorta ratio (p<0.001). Ascites was found in 4 CP+ patients.

Liver relaxometry (Table 2)

Native T1 and T2 values of the liver were significantly higher in CP+ than in CP- patients or control subjects, i.e. T1: 765±102ms, 581±56ms and 537±29ms (p<0.001), T2: 63±13ms, 50±4ms, 46±4ms (p<0.001)(Figure 1 and 2). Moreover, ECV values were higher in CP+ than in CP- patients and controls i.e. 41±7%, 31±3 % and 30±3%, respectively (p<0.001). Native T1 values correlated well with T2 and ECV values, i.e. R^2 of 0.76 and 0.72, respectively, while T2 values correlated moderately with ECV value, i.e. R^2 of 0.58 (all p<0.001)(Supplementary Figure 1). Moreover, GGT correlated well with native T1 liver (r^2=0.43, p<0.001) and ECV liver (r^2=0.30, p<0.001), weakly with T2 liver (r^2=0.18, p<0.001)(Supplementary Figure 2). Using RA pressure as reference (i.e. RA pressure > 5 mm Hg), native T1 of the liver yielded the highest area under the curve (AUC) at receiver operating characteristic (ROC) analyses (0.926) yielding a sensitivity and specificity of specificity of 79.3% and 95.6%, respectively, to differentiate between normal and increased RA pressure (Figure 3, 4). Both native T1 and T2 (AUC: 0.868) of the liver were not significantly different from GGT (AUC: 0.868) but performed better than total bilirubin (AUC: 0.766) (p<0.05). In figure 5 is shown an example of important congestive hepatopathy with normalization after anti-inflammatory therapy.

Intra- and inter-observer agreement for native T1, T2 liver and ECV liver was excellent with all ICC values above 0.9, and a CV ranging from 3.1% to 8.3% and 2.2% to 10.0% for intra-observer and inter-observer agreement, respectively (table 3).

Discussion

To summarize, in the present study we showed that in constrictive pericarditis patients, assessment of relaxation values of the liver parenchyma on routinely acquired T1 and T2 maps of the heart may provide valuable and reproducible information with regard to the presence of passive liver congestion, reflecting increased right heart filling pressures caused by pericardial constriction. Findings at liver mapping correlated significantly with serum liver biomarkers, in particular GGT, which is deemed to reflect elevated RA pressures (4,5). As filling pressure pressures cannot be measured at cardiovascular MR imaging, information obtained by liver mapping may be valuable to indirectly depict right heart failure in pericarditis patients.

The diagnosis of constrictive pericarditis is typically two-fold, i.e. firstly, depiction of a pathologic non-compliant pericardium; secondly, demonstration of constrictive physiology. Presence of a rigid pericardium, impeding cardiac filling, causes increased filling pressures and symptoms of congestive heart failure [9-11]. Moreover, the ventricular (inter)dependence (or coupling) is increased and enhanced by respiration. The latter is a pathognomonic hallmark of constrictive pericarditis allowing differentiation with restrictive cardiomyopathy. In recent years, cardiovascular MR imaging has become an important modality in the diagnosis of constrictive pericarditis, as it allows not only an excellent assessment of the pathologic pericardium (e.g. thickness, presence of pericardial edema, pericardial enhancement, effusion) but also depicting of abnormal ventricular coupling [9-11]. However, assessment of congestive heart failure is more challenging as filling pressures cannot be measured at cardiovascular MR imaging. As the liver immediately feels the adverse effects of increased right heart pressures, assessment of this target organ provides valuable information on the presence of congestive heart failure. As shown in the present study, assessment of T1 and T2 relaxation times and ECV maps of the liver parenchyma using the T1, T2 and ECV maps of the myocardium provides valuable information on the presence of passive liver congestion, without prolonging scanning time or adding time-consuming post-processing. On the contrary, it enhances the clinical role of cardiovascular MR imaging as it allows a better appreciation of the patient's hemodynamic status.

As mentioned above, MR relaxometry has dramatically changed our understanding of cardiac diseases by allowing for quantitative and precise imaging of myocardial tissue abnormalities which enable to evaluate disease progression and response to therapy [12,13]. So far, the main focus of MR relaxometry has been myocardial texture analysis, though some preliminary reports suggest the utility to assess other organs. For instance, splenic relaxation times have been applied with success to assess of the response to adenosine during stress perfusion cardiovascular MR imaging [14]. In contrast, relaxometry of the liver in cardiac patients has received limited interest. Preliminary results suggested that mapping of the liver may be useful in patients with tetralogy of Fallot and in Fontan circulation [15,16]. Our findings not only endorse those findings but suggest a broader use of liver MR relaxometry offering valuable information in cardiac conditions which affect the liver with potential deleterious consequences, such as cardiac cirrhosis.

The liver-to-heart axis becomes important into two main contexts: 1) severely impaired cardiac output leading to peripheral organs hypoperfusion (e.g. cardiogenic shock); 2) increased central venous pressure

due to inability of the right heart to accommodate the venous return [1,2,17]. In our study, none of the patients had impaired cardiac output, thereby liver hypoperfusion can be easily ruled out. Moreover, primary liver diseases (e.g., hepatitis) were careful excluded by thorough assessment of the clinical records. Thus, the increased values at MR relaxometry of the liver reflect an increased central venous pressure due to constrictive physiology prompted by pericarditis. Patients with pericarditis and increased ventricular coupling, deemed to reflect constrictive physiology, show not only signs of increased filling pressures at TTE (dilated IVC with diminished/absent respiratory motion, increased RA pressure) and cardiovascular MR imaging (dilated IVC, with increased IVC/aorta ratio, dilated hepatic veins, ascites), but show significantly longer T1 and T2 relaxation time of the liver coupled with higher ECV as compared to pericarditis patients with normal ventricular coupling or controls. Of interest, T1 value of the liver, and to a lesser extent ECV, correlated well with liver enzymes, in particular cholestatic enzymes such as GGT. These observations point toward the use of MR relaxometry as imaging biomarker to depict congestive hepatopathy.

Whereas MR relaxometry of the liver has hardly been used in cardiac patients, use of this modality is more common in patients with ‘primary’ liver pathology such as to liver fibrosis in the setting of chronic hepatitis and cirrhosis, and hemochromatosis [18,19]. Of note, the values in our healthy control group agree well with normal values in literature [20,21]. Moreover, MR relaxometry has been compared to MR elastography in patients with liver fibrosis/cirrhosis and shown a good correlation between these techniques [18,19]. Of interest, in an animal model of liver congestion, changes in RA pressure have an immediate effect on the liver [7]. In patients with constrictive pericarditis, Fenstad et al. showed increased liver stiffness, correlating with septal bounce, IVC size and abnormal septal motion [22]. These findings suggest that liver relaxation times can be used as an alternative to MR elastography to appreciate hepatic venous congestion and/or fibrosis, which is appealing as the time-consuming MR elastography (i.e. extra measurement time about 20 minutes) may be too long to add in patients with right heart failure [6].

Limitations. *Firstly*, because of the retrospective nature, this paper is to a large extent descriptive. As congestive hepatopathy reflects a wide spectrum ranging from pure congestion to onset of liver fibrosis eventually leading to cardiac cirrhosis [1-3] the current study findings do not provide information on the histologic correlate as no liver biopsy was performed, nor on the reversibility of findings as most patients did not undergo a follow-up cardiovascular MR imaging. *Secondly*, in a small number of patients routinely cardiac mapping did not sufficiently encompass the liver parenchyma (i.e. less than 10% in our study). In these patients additional imaging, e.g. coronal of transverse liver imaging, may be recommended. *Thirdly*, positioning of the T1 and T2 sequences for cardiac mapping and local shim volume may be suboptimal to study the liver parenchyma. To deal with this potential issue, the region of interest to measure liver relaxation times was selected as close as possible to the heart. *Finally*, only in constrictive pericarditis patients who underwent pericardiectomy right heart catheterization with pressure measurements was performed, while in the other subjects, the RA pressure was estimated by echocardiography which may be less accurate. descriptive.

In conclusion, liver mapping as part of a comprehensive cardiovascular MR imaging exam may provide valuable information with regard to the presence of congestive hepatopathy in constrictive pericarditis patients. The current study findings open perspectives towards a more generalized use of liver MR relaxometry in cardiac patients, in particular in those at risk of developing right heart failure.

Methods

Study population.

A search in our cardiovascular MR imaging database (2014-2020) yielded 337 patients with MR diagnosis suggestive of pericarditis. Incomplete studies (n=51) or studies with insufficient coverage of the liver parenchyma of the T1/T2 maps (n=25) were excluded. Next, patients with concomitant liver pathology (e.g. liver cirrhosis) were excluded (n=12). This yielded 249 cardiovascular MR studies. In 25 studies (10%), increased ventricular coupling was found at free-breathing real-time cine MR imaging, defined as inspiratory septal inversion, and/or increased excursion of the ventricular septum between inspiration and expiration [11]. These patients were defined as pericarditis with constrictive physiology (*CP+group*). We randomly selected 20 patients in the cohort without increased ventricular coupling and defined them as pericarditis without constrictive physiology (*CP- group*). Finally, we selected as control group 30 subjects with normal cardiovascular MR imaging findings, lack of increased central venous pressure at TTE and normal liver enzymes (*control group*). The study was conducted in accordance with the Declaration of Helsinki and was approved by the research ethics committee of the hospital. Because of the retrospective design, informed consent by the patient was waived.

MR imaging protocol.

Studies were performed on a 1.5T scanner (Ingenia, Philips Healthcare). The protocol consisted of scout images, T1 and T2 weighted fast spin-echo imaging, breath-hold steady-state free precession (SSFP) cine imaging along the different cardiac axes, T1 and T2 myocardial mapping, late gadolinium enhancement (LGE) imaging and post-contrast T1 mapping, and free breathing real-time imaging in midventricular cardiac short-axis to assess ventricular coupling. *T1-weighted imaging* was performed using a T1-weighted black-blood turbo spin-echo (TSE) in cardiac short-axis. Typical imaging parameters were flip angle, 90°; TR/TE 1 beats/8.6 ms; sense factor, 2.1; TSE factor, 24 with asymmetric profile order; matrix 320x266; FOV, 320x266 mm (incl. fold-over suppression, 380 mm); slice thickness, 8 mm; acquired resolution, 1.05x1.32 mm; reconstructed resolution, 0.5x0.5mm; phase percentage, 70-80%, bandwidth, 490 Hz, and black blood preparation (TI 180 ms) and thickness 20 mm. The ventricles were completely encompassed using 6 to 10 slices (variable gap). *T2-weighted imaging* was performed using a black blood short-tau inversion-recovery (STIR) turbo spin-echo (TSE) in cardiac short-axis. Typical imaging parameters were TR/TE 2 beats/85 ms; sense factor, 2; TSE factor, 33 with linear profile order; halfscan factor, 0.8; matrix 256x164; FOV, 320x280 mm (incl. fold-over suppression, 560 mm); slice thickness, 8 mm; acquired resolution, 1.4x1.7 mm; reconstructed resolution, 0.7x0.7 mm; phase percentage, 70-80% and black blood inversion preparation (TI 180 ms) and thickness 20 mm. The ventricles were completely

encompassed using a slice gap of 2 mm. For assessment of LV dimensions and function *balanced SSFP breath-hold cine images* were acquired in the following orientations: vertical and horizontal long-axis, short-axis and left ventricular (LV) outflow tract view. Typical imaging parameters were: repetition time (TR) / echo time (TE), shortest/shortest (e.g. 3.6/1.8 ms); sense factor, 2 or compressed sense (CS), 2.5; halfscan factor, 0.625; flip angle, 60°; matrix 208x160; field of view (FOV) 350x274 mm (with fold-over suppression 360 mm); acquired resolution, 1.7x1.7 mm; reconstructed resolution, 1.0x1.0 mm; slice thickness, 8 mm; pixel bandwidth, 954 Hz, and number of phases, 30, phase percentage, 67%. In cardiac short-axis, the left ventricle was encompassed completely using a slice gap of 2 mm. These cine MRI images were acquired starting from one minute post-contrast administration, followed by a three-chamber cine view using similar sequence parameters as above. *LGE cardiovascular MR imaging* was performed using a breath-hold 3D turbo-field-echo inversion recovery sequence (IR-TFE) and/or phase-sensitive inversion-recovery (PSIR) sequence in short-axis, vertical and horizontal long-axis. LGE was started 10 minutes after injection of 0.15 mmol/kg of commercially available gadolinium-chelates (gadobutrol, Gadovist Bayer). Typical imaging parameters: TR/TE, shortest/shortest; sense factor, 2 or CS, 6.5; matrix sense 256x164 or CS 168x159; FOV, sense 350x350 or CS 320x320; acquired resolution, sense, 1.4x2.2x10mm or CS, 1.9x2.0x10mm; reconstructed, 1.3x1.3x5mm; flip angle, 15°. A Look-Locker sequence was used to determine the optimal inversion time to null myocardium (IR-TFE) or blood (PSIR*). T1 mapping* images were acquired in 4-chamber long-axis and midventricular (in most also basal and apical) 2D short-axis orientations using the modified look-locker inversion recovery (MOLLI) sequence. For native T1 mapping MOLLI we used a 5s(3s)3s protocol (hsec inv pulse, minimum inversion times 110 and 350ms, balanced SSFP readout with TR:2.0ms, TE:0.9ms, flip angle: 35°, slice thickness: 10mm, acquisition matrix: 152x150 reconstructed to 256x256, SENSE factor: 2, BW: 1082 Hz, FOV: 300x300mm, pixel size: 2.0x2.0mm, reconstructed pixel size 1.2x1.2mm). At 10 min T1 mapping was repeated using a 4s(1s)3s(1s)2s protocol (minimum inversion times about 110, 230 and 350ms, all other parameters as for MOLLI native). *T2 mapping* was performed using a gradient-echo spin-echo sequence (GRASE) (9 echoes with TE:10-100 ms, TR/TE, 1 beat/shortest; sense factor,2; matrix 152x139; FOV, 300x300mm (with fold-over suppression 420 mm); slice thickness, 10 mm; acquired resolution, 2.0x2.0 mm; reconstructed resolution, 1.0x1.0 mm). Typically, 3 short-axis T2 maps were obtained covering basal, mid and apical part of the LV. Finally, *real time cines images* were acquired over 250 dynamics during deep respiration using a single-shot balanced TFE sequence with specific parameters: repetition time (TR) / echo time (TE), shortest/shortest (e.g. 1.9/0.8 ms); sense factor, 2; halfscan factor, 0.625; flip angle, 50°; matrix 96x65; FOV 360x304 mm (no fold-over suppression); acquired resolution, 3.8x4.7 mm; reconstructed resolution, 2.5x2.5 mm; slice thickness, 10 mm; pixel bandwidth, 3519 Hz.

MR analysis.

Images were analyzed off-line using IntelliSpace Portal software (Philips Healthcare) by an European Association Cardiovascular Imaging (EACVI) level-III CMR reader. Pericardial thickness was measured, and the images were assessed for presence of effusion, edema (T2-weighted imaging) and inflammation (LGE imaging). Cine images were used to calculate LV and right ventricular (RV) volumes, function, and LV mass. Left atrial and right atrial area was contoured on the end-systolic horizontal long-axis image.

The diameter of the IVC and descending aorta were measured at the level of the diaphragm. Hepatic vein size was visually assessed as normal or dilated. Presence of pleural fluid and ascites were evaluated. The early-diastolic inspiratory shape of the ventricular septum was described at real-time cine imaging as normal, flattened or inverted, and the total shift of the septum between inspiration and expiration was measured [11]. As mentioned above, this information was used to define the CP+ and CP- group.

On the T1 and T2 map, myocardial T1 and T2 was measured in the ventricular septum, and a standardized method was used to calculate myocardial ECV. For the liver, a region of interest (ROI) was drawn freehand with a minimum number of 500 pixels. The ROI was typically chosen in the subcapsular liver parenchyma in the vicinity of the heart. Care was taken not to include the centrally located liver vessels. A similar formula as for the myocardium was used to calculate ECV liver (23), but the RV cavity instead of the LV cavity was used to measure the T1 of blood. Intra- and inter-reader reproducibility of T1/T2 liver mapping was assessed in 30 randomly chosen patients (10 from each group).

Statistical analysis

Statistical analysis was performed using R programming language for statistical computing v.4.0.0. (The R-Foundation for Statistical Computing). Histograms and Q-Q plots with graphical bootstrap were used to test the normality of the data distributions. Continuous variables were expressed as mean ± SD or medians with interquartile ranges (IQR) as appropriate. Categorical variables were expressed as frequency with percentage. One-way analysis of variance (ANOVA) or the Kruskal-Wallis test were used to assess differences among the different groups, and post hoc pairwise comparisons with Bonferroni adjustment were performed by using the Student t test or Wilcoxon Rank Sum test, respectively. The Chi-square test or Fisher's exact test was used to compare categorical variables. ROC curve analysis was performed to examine differences in performance of each variable for prediction of clinical symptoms of RHF (i.e., elevated central venous pressure, lower limb edema, NYHA class >2). The 95% confidence interval (CI) of each area under the curve (AUC) was estimated and compared with the R "pROC" package using the DeLong method [24]. The optimal cut-off points for each continuous predicator was defined from the ROC analysis in terms of maximum sensitivity and specificity by using the Youden index [25]. The Youden index (J) is defined as , with J=1 indicating complete separation and J=0 indicating complete overlap of distributions. The amount of overlap in values among different patient group was assessed using density plots and quantified using the R "overlapping" package with bootstrap estimates [26]. An adjusted 2-tailed p-value <0.05 was considered to indicate a statistically significant difference. Intra-reader and inter-reader agreement of multiparametric liver mapping were assessed by using intraclass correlation coefficients (ICCs) and Bland-Altman analysis with 95% limits of agreement (LOAs). ICCs of greater than 0.75 and of 0.4-0.75 indicate strong and average agreement, respectively. A difference between ICCs was considered to be statistically significant when there was no overlap between their respective 95% CI limits.

Human subject research.

This retrospective, observational study was approved by the Ethics Committee Research UZ/KU Leuven (S64242). Because of the retrospective design, informed consent by the patient was waived by the Ethics Committee Research UZ/KU Leuven.

Declarations

Competing Interests

The authors declare no competing interests.

Data availability.

Data generated for analysis during this study are included in this published article.

Author Contributions

Conception and design of study: J.B., R.S., M.I., P.G.M. Acquisition of data (laboratory or clinical): J.B., L.T., P.S., R.S. Data analysis and/or interpretation: J.B., R.S., T.D., P.S., P.G.M., M.I. Drafting of manuscript and/or critical revision: J.B., T.D., L.T., P.S., P.M., M.I., R.S. All authors read and approved the final manuscript.

References

1. El Hadi, H., Di Vincenzo, A., Vettor, R. & Rossato, M. Relationship between heart disease and liver disease: a two-way street. *Cells***9**,567, https://doi:10.3390/cells9030567 (2020).
2. Megalla, S. *et al*. Predictors of cardiac hepatopathy in patients with right heart failure. *Med Sci Monit***17**,CR537-541, https://doi.org/10.12659/MSM.881977 (2011).
3. Wells, M.L. *et al*. Imaging findings of congestive hepatopathy. *RadioGraphics***36**,1024-1037, https://doi:1148/rg.2016150207 (2016).
4. van Deursen, V.M. *et al.* Abnormal liver function in relation to hemodynamic profile in heart failure patients. *J Cardiac Failure***16**,84-90, https://doi.org/10.1016/j.cardfail.2009.08.002 (2010).
5. Ess, M. *et al.* Gamma-glutamyltransferase rather than total bilirubin predicts outcome in chronic heart failure. *J Cardiac Failure***17**,577-584, https://doi.org/10.1016/j.cardfail.2011.02.012 (2011).
6. Huwart, L. *et al.* Liver fibrosis: noninvasive assessment with MR elastography versus aspartate aminotransferase-to-platelet ratio index. *Radiology***245**,458-466, https://doi.org/10.1148/radiol.2452061673 (2007).
7. Millonig, G. *et al.* Liver stiffness is directly influenced by central venous pressure. *J Hepatol* **52**,206-210, https://doi.org/10.1016/j.jhep.2009.11.018 (2010).
8. Taniguchi, T. *et al.* Liver stiffness reflecting right-sided filling pressure can predict adverse outcomes in patients with heart failure. *J Am Coll Cardiol Img***12**,955-964, https://doi.org/10.1016/j.jcmg.2017.10.022 (2019).

9. Adler, Y. *et al.* 2015 ESC Guidelines for the diagnosis and management of pericardial diseases: the Task Force for the diagnosis and management of pericardial diseases of the European Society of Cardiology (ESC) endorsed by: the European Association for Cardio-Thoracic Surgery (EACTS). *Eur Heart J***36**,2921-2964, https://doi.org/10.1093/eurheartj/ehv318 (2015)
10. Chetrit, M. *et al.* Imaging-guided therapies for pericardial diseases. *J Am Coll Cardiol Img***13**,1422-1437, https://doi.org/10.1016/j.jcmg.2019.08.027 (2020).
11. Francone, M. *et al.* (2006) Assessment of ventricular coupling with real-time cine MRI and its value to differentiate constrictive pericarditis from restrictive cardiomyopathy. *Eur Radiol***16**:944-951, 1007/s00330-005-0009-0 (2006).
12. Moon, J.C. *et al.* Society for Cardiovascular Magnetic Resonance Imaging: Cardiovascular Magnetic Resonance Working Group of the European Society of Cardiology. Myocardial T1 mapping and extracellular volume quantification: a Society for Cardiovascular Magnetic Resonance (SCMR) and CMR Working Group of the European Society of Cardiology consensus statement. *J Cardiovasc Magn Reson***15**:92, https://doi.org/10.1186/1532-429x-15-92 (2013).
13. Ugander, M. *et al.* Myocardial edema as detected by pre-contrast T1 and T2 CMR delineates area at risk associated with acute myocardial infarction. *J Am Coll Cardiol Imag***5**:596-603, https://doi.org/10.1016/j.jcmg.2012.01.016 (2012).
14. Liu, A. *et al.* Splenic T1-mapping: a novel quantitative method for assessing adenosine stress adequacy for cardiovascular magnetic resonance. *J Cardiovasc Magn Reson***19**,1, https://doi.org/10.1186/s12968-016-0318-2 (2017).
15. Kazour, I. *et al.* Using T1 mapping in cardiovascular magnetic resonance to assess congestive cardiomyopathy. *Abdom Radiol***43**,2679-2685, https://doi.org/10.1007/s00261-018-1528-x (2018).
16. de Lange, C. *et al.* Increased extracellular volume in the liver of pediatric Fontan patients. *J Cardiovasc Magn Reson***21**,39, https://doi.org/10.1186/s12968-019-0545-4 (2019).
17. Konstam, M.A. *et al.* Evaluation and management of right-sided heart failure. A scientific statement from the American Heart Association. *Circulation***137**,e578-e622, https://doi.org/10.1161/cir.0000000000000560 (2018).
18. Li, J. *et al.* Native T1 mapping compared to ultrasound elastography for staging and monitoring liver fibrosis: an animal study of reproducibility, and accuracy. *Eur Radiol***30**,337-345, https://doi.org/10.1007/s00330-019-06335-0 (2020).
19. Banerjee, R. *et al.* Multiparametric magnetic resonance for the non-invasive diagnosis of liver disease. *J Hepatology***60**,69-77, https://doi.org/10.1016/j.jhep.2013.09.002 (2014).
20. de Bazelaire, C.M.J. *et al.* MR imaging relaxation times of abdominal and pelvic tissues measured in vivo at 3.0T: preliminary results. *Radiology***230**,652-659, https://doi.org/10.1148/radiol.2303021331(2004).
21. Gilligan, L.A. *et al.* Magnetic resonance imaging T1 relaxation times for the liver, pancreas and spleen in healthy children at 1.5 and 3 Tesla. *Pediatr Radiol***49**,1018-1024, https://doi.org/10.1007/s00247-019-04411-7 (2019).

22. Fenstad, E.R. *et al.* Evaluation of liver stiffness with magnetic resonance elastography in patients with constrictive pericarditis: preliminary findings. *J Magn Reson Imaging* **44**:81-88, https://doi.org/10.1002/jmri.25126 (2016).
23. Kellman, P., Wilson, J.R., Xue, H., Ugander, M. & Arai, A.E. Extracellular volume fraction mapping in the myocardium, part : evaluation of an automated method. J Cardiovasc Magn Reson 14,63, https://doi.org/10.1186/1532-429x-14-63 (2012).
24. DeLong, E.R., DeLong, D.M. & Clarke-Pearson, D.L. Comparing the areas under two or more correlated receiver operating characteristic curves: a nonparametric approach. Biometrics. *JSTOR* **44**,837–845, (1988).
25. Fluss, R., Faraggi, D. & Reiser, B. Estimation of the Youden Index and its associated cutoff point. *Biometrical J* **47**,458–472, https://doi.org/10.1002/bimj.200410135 (2005).
26. Pastore, M. Overlapping: a R package for estimating overlapping in empirical distributions. *J Open Source Softw* **3**,1023, (2018).

Tables

Table 1 – Clinical presentation, laboratory results, transthoracic echocardiography and right heart catheterization

	CP+ Group (n=25)	CP- Group (n=20)	Control (n=30)	p-value
Clinical presentation				
- age (y)	59 ± 15	46 ± 15*	47 ± 13*	0.003
- male gender (%)	22 (88)	18 (90)	15 (50)*,**	<0.001
- BSA (m^2)	1.97 ± 0.26	1.96 ± 0.19	1.86 ± 0.19	0.09
- heart rate (bpm)	82 ± 12	69 ± 12*	62 ± 11*	<0.001
- SBP (mm Hg)	122 ± 20	121 ± 12	127 ± 19	0.41
- DBP (mm Hg)	75 ± 11	76 ± 8	76 ± 9	0.90
- NYHA class ≥2	20 (80)	3 (15)*	1 (3)*	<0.001
- edema lower limbs (%)	9 (36)	0 (0)*	0 (0)*	<0.001
- CVP increase (%)	13 (52)	0 (0)*	0 (0)*	<0.001
- pericarditis like pain (%)	9 (36)	19 (95)*	0 (0)*,**	<0.001
- atrial fibrillation (%)	6 (24)	2 (10)	0 (0)*	0.004
Laboratory values				
- CRP (mg/l)	28.9 (5.8-60.0)	32.0 (5.2-119.5)	0.8 (0.5-1.0)*,**	<0.001
- troponin I (µg/l)	0.019 (0.011-0.038)	0.006 (0.004-0.010)*	0.004 (0.003-0.005)*,**	<0.001
- hematocrit (%)	38.3 ± 5.4	41.0 ± 5.5	43.0 ± 2.7*	0.001
- GGT (U/l)	103 (59-155)	25 (19-34)*	19 (13-27)*	<0.001
- AST (U/l)	27 (22-33)	21 (14-28)	19 (16-22)*	0,008
- ALT (U/l)	22 (19-34)	21 (17-31)	21 (14-27)	0.32
- alkaline phosphatase (U/l)	115 (94-138)	75 (59-95)*	68 (61-76)*	<0.001
- bilrubin total (mg/dl)	0.62 (0.41-0.89)	0.37 (0.23-0.50)*	0.42 (0.34-0.47)*	0.006
- LDH (U/l)	208 (183-239)	186 (160-213)	177 (166-195)	0.06
- creatinine (mg/dl)	1.01 (0.93-1.17)	0.96 (0.89-1.19)	0.78 (0.73-0.89)*,**	<0.001

- eGFR (ml/min/1.73m^2)	84 (64-96)	83 (70-90)	90 (86-99)*,**	0.006
TTE findings				
- E/A	1.4 (1.1-1.7)	1.3 (1.0-1.7)	1.6 (1.3-1.7)	0.50
- E/E'	7.6 (6.3-9.3)	6.6 (5.2-8.2)	7.1 (5.7-8.2)	0.53
- IVC dilated (%)	17 (68)	1 (5)*	0 (0)*	<0.001
- IVC absent resp. variation (%)	20 (80)	1 (5)*	0 (0)*	<0.001
- RA pressure (mmHg)	15 (10-15)	5 (5-10)*	5 (0-5)*	<0.001
Right heart catheterization				
- RA pressure (mm Hg)	20 (18-22)			NA
* = post hoc significant vs CP+ group				
** = post hoc significant vs CP- group				

Table 2 – MR Imaging findings

	CP+ Group (n=25)	CP- Group (n=20)	Control (n=30)	p-value
Left ventricle				
- EDV indexed (ml/m^2)	57 ± 15	80 ± 17 *	83 ± 15*	<0.001
- ESV indexed (ml/m^2)	25 ± 8	34 ± 10 *	34 ± 9 *	<0.001
- SV indexed (ml/m^2)	32 ± 10	46 ± 9 *	49 ± 8 *	<0.001
- EF (%)	56 ± 8	58 ± 7	59 ± 5	0.14
Right Ventricle				
- EDV indexed (ml/m^2)	58 ± 14	80 ± 18 *	82 ± 16 *	<0.001
- ESV indexed (ml/m^2)	28 ± 8	36 ± 11 *	33 ± 9	<0.001
- SV indexed (ml/m^2)	30 ± 9	44 ± 11 *	48 ± 9 *	<0.001
- EF (%)	52 ± 9	57 ± 7 *	58 ± 6 *	0.005
Atria				
- LA indexed (cm^2/m^2)	13 ± 2	11 ± 2	11 ± 2	0.07
- RA indexed (cm^2/m^2)	11 ± 2	12 ±2	11 ± 1	0.98
Myocardium & blood				
- native T1 myocardium (ms)	1011 ± 22	1002 ± 29	999 ± 22	0.14
- T2 myocardium (ms)	51 ± 3	52 ± 2	51 ± 3	0.73
- ECV myocardium (%)	27.9 ± 3.8	25.6 ± 2.4 *	25.0 ± 2.4 *	0.003
- native T1 blood (ms)	1636 ± 109	1541 ± 69 *	1513 ± 70 *	<0.001
Liver				
- native T1 liver (ms)	765 ± 102	581 ± 56 *	537 ± 30 *	<0.001
- T2 liver (ms)	63 ± 13	50 ± 4 *	46 ± 4 *	<0.001
- ECV liver (%)	42 ± 7	31 ± 3 *	30 ± 3 *	<0.001
Pericardium				
- pericardial thickness (mm)	5.0 (4.0 - 11.0)	1.7 (1.3 - 3.4) *	1.1 (1.0 - 1.3) *	<0.001

- pericardial enhancement (%)	23 (92)	20 (100)	0 (0) *,**	<0.001
- inspiratory septal inversion (%)	15 (60)	0 (0) *	0 (0) *	<0.001
- respiratory septal shift (%)	20 (15 - 27)	7 (5 - 8) *	7 (6 – 8) *	<0.001
Other				
- ratio diameter IVC/aorta	1.26 ± 0.24	1.04 ± 0.21 *	0.99 ± 0.13 *	<0.001
- pleural effusion (%)	20 (80)	4 (20) *	0 (0) *	<0.001
- dilated hepatic veins (%)	15 (60)	0 (0) *	0 (0) *	<0.001
- ascites (%)	4 (16)	0 (0)	0 (0)	0.01
* = post hoc significant vs CP+ group				
** = post hoc significant vs CP- group				

Table 3 – Intra-reader and inter-reader agreement

	Intra-reader agreement			Inter-reader agreement		
	ICC	**95% CI**	**CV**	**ICC**	**95% CI**	**CV**
T1 liver	0.983	0.965-0.992	3.1	0.991	0.982-0.996	2.2
T2 liver	0.967	0.933-0.984	4.5	0.944	0.887-0.973	6.3
ECV liver	0.928	0.856-0.965	8.3	0.900	0.802-0.951	10.0

Figures

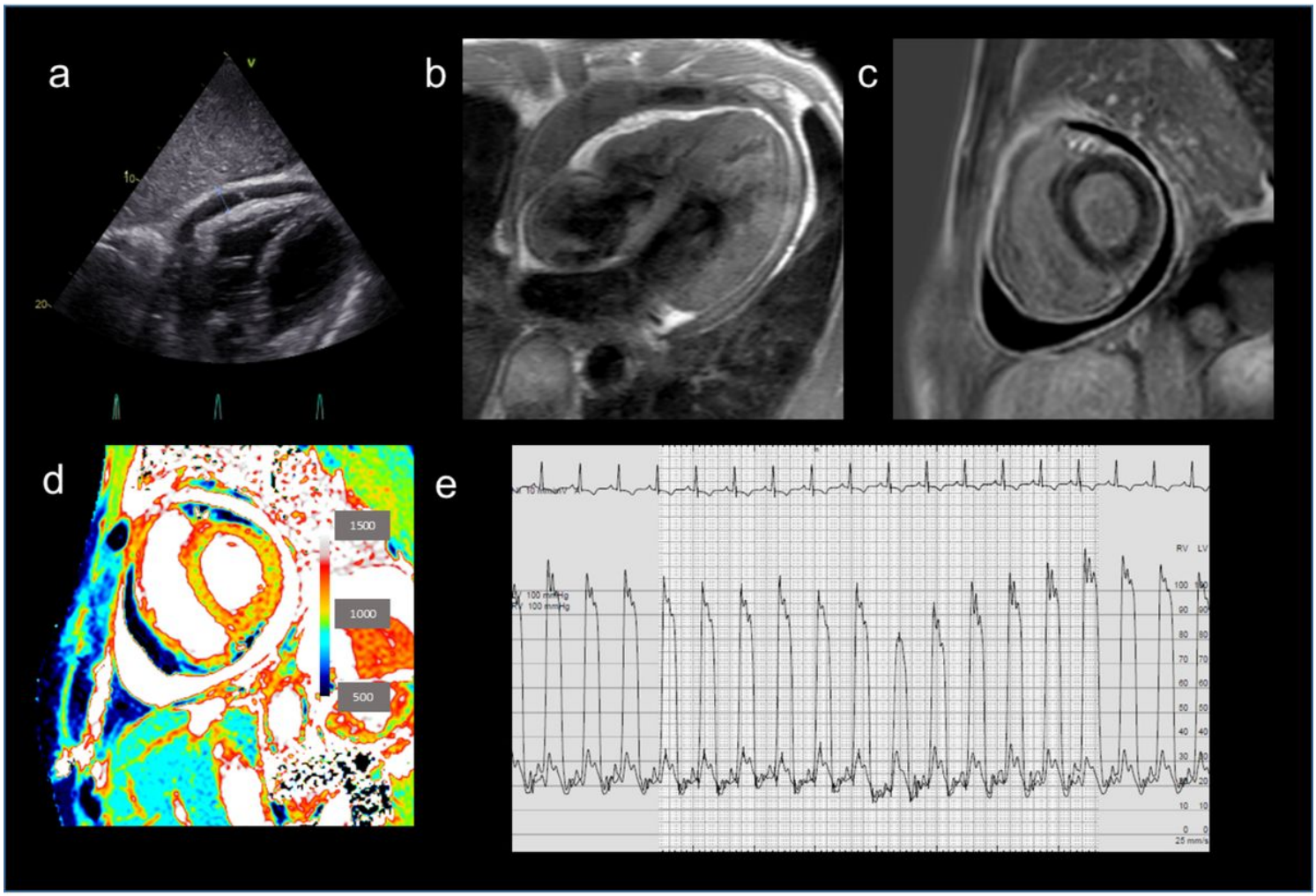

Figure 1

Inflammatory-effusive pericarditis with constrictive physiology. 37-year-old man with viral syndrome for 3 weeks, malaise and fatigue but no fever nor chest pain. Raise in CRP (64 mg/l) and isolated increase in GGT (126 U/L). TTE showed moderate pericardial effusion with increased ventricular coupling (panel a, video 1a), dilated IVC with absent respiratory variation (video 1b) and expiratory diastolic flow reversal in hepatic veins. Cardiovascular MR imaging showed moderate pericardial effusion with thickened contrast-enhancing pericardial layers (panel b,c) and pronounced S-like ventricular septal motion (video 1c). Free

breathing cine MR imaging showed early-diastolic, inspiratory ventral septal inversion with increased ventricular septal shift (32%)(video 1d). Increased T1 liver (837 ms), T2 liver (67 ms), and ECV liver (55.6%) values. Presence of bilateral pleural effusion. Right heart catheterization showed increased RA pressures (18 mm Hg), pressure equalization with dip and plateau curve (panel d). The patient underwent successfully a pericardiectomy. Histology showed a fibrous thickened pericardium with fibrinous inflammation without evidence of acute inflammation nor granulomata.

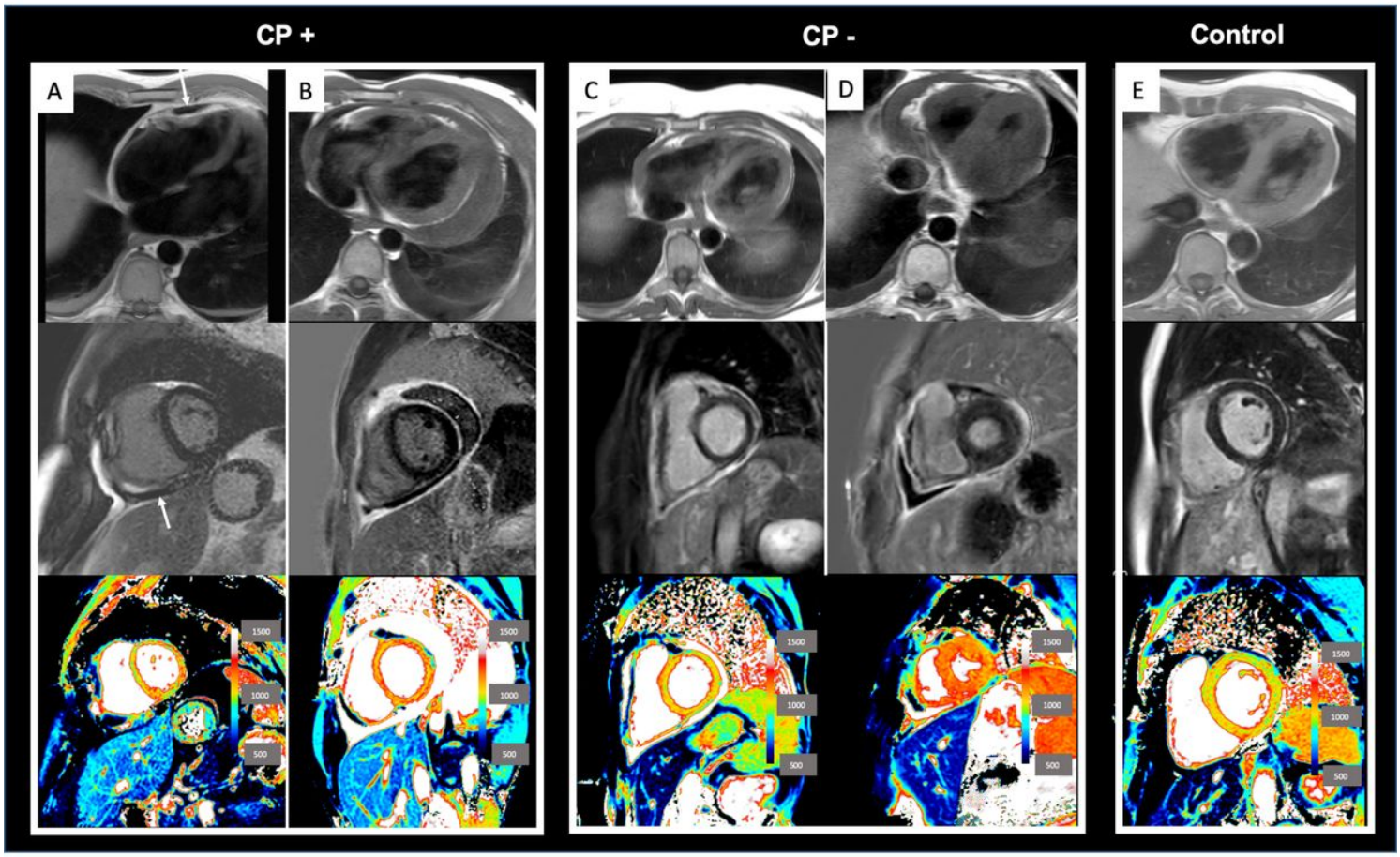

Figure 2

Comparison of congestive hepatopathy in CP+, CP- cohort and Control Group CP+ group: healed (“end-stage”) constrictive pericarditis (A), inflammatory-effusive constrictive pericarditis (B). CP- group: dry inflammatory pericarditis (C), inflammatory-effusive pericarditis without constrictive physiology (D). Control subject (E). Axial T1-weighted fast spin-echo image (upper row), cardiac short-axis LGE (middle row), and pre-contrast T1 map (lower row). While normal T1 values of the liver are visually shown on the color-coded maps as dark blue, increased T1 values range from light blue to green/yellow (see also Figure 5). Numerical T1 liver values: 779 ms (A), 738 ms (B), 547 ms (C), 638 ms (D), and 575 ms (E). The white arrow in patient A indicates a thickened, fibrotic pericardium.

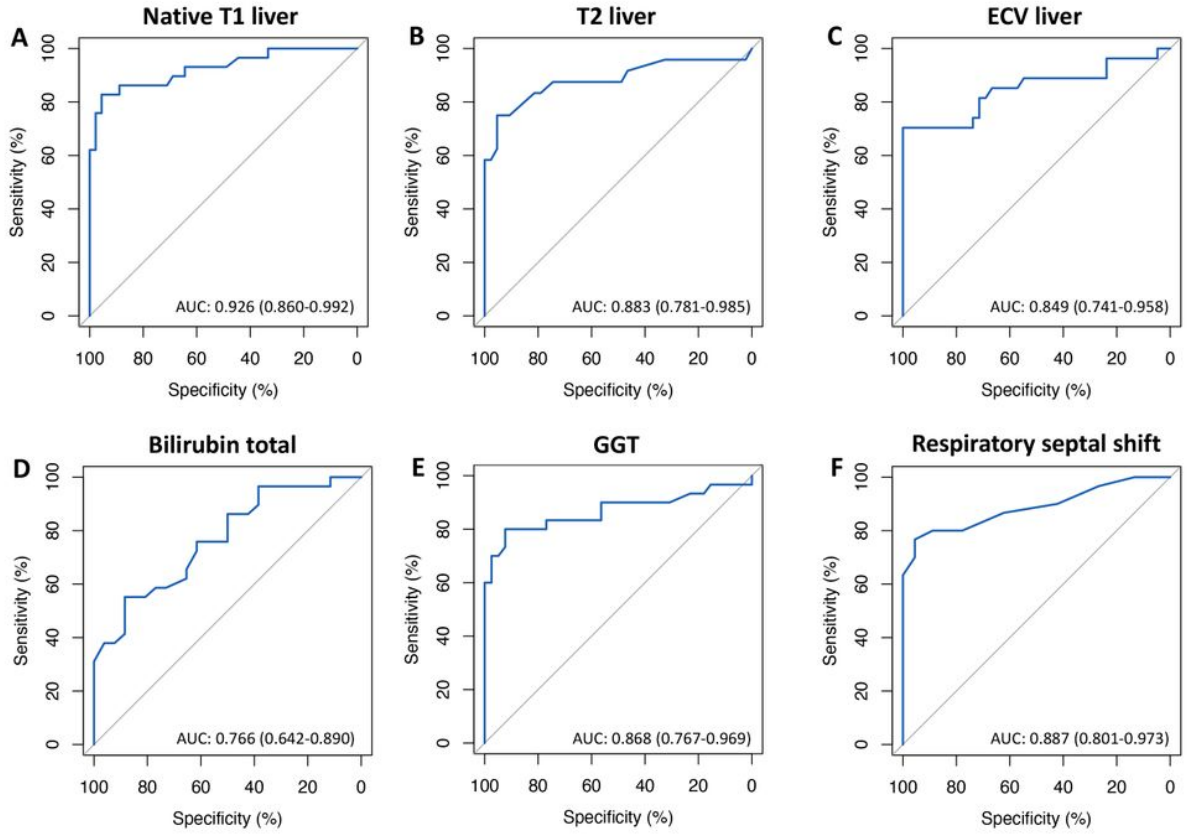

Figure 3

ROC curves to assess increased RA pressure

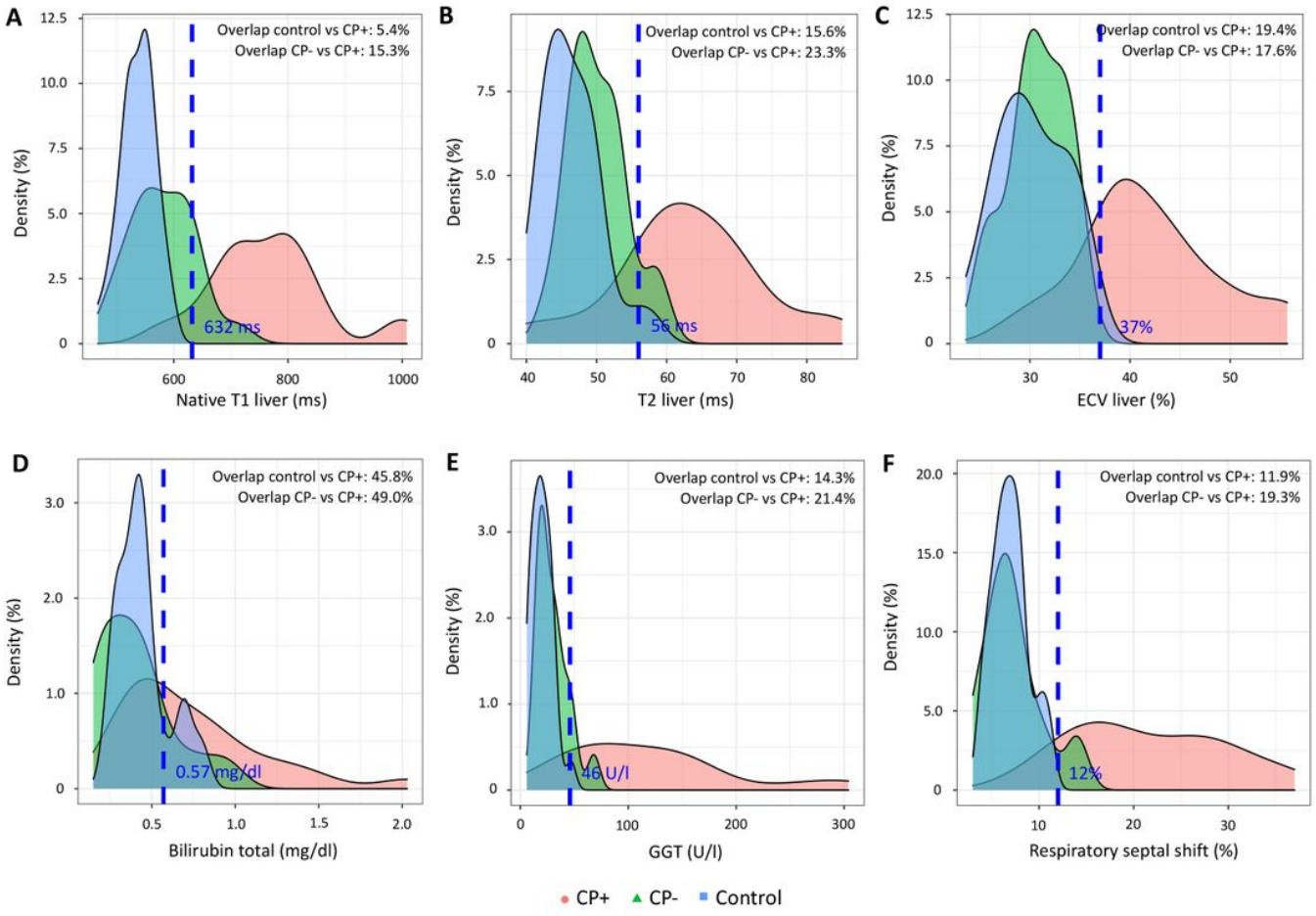

Figure 4

Density plots to discriminate between presence/absence of increased RA pressure

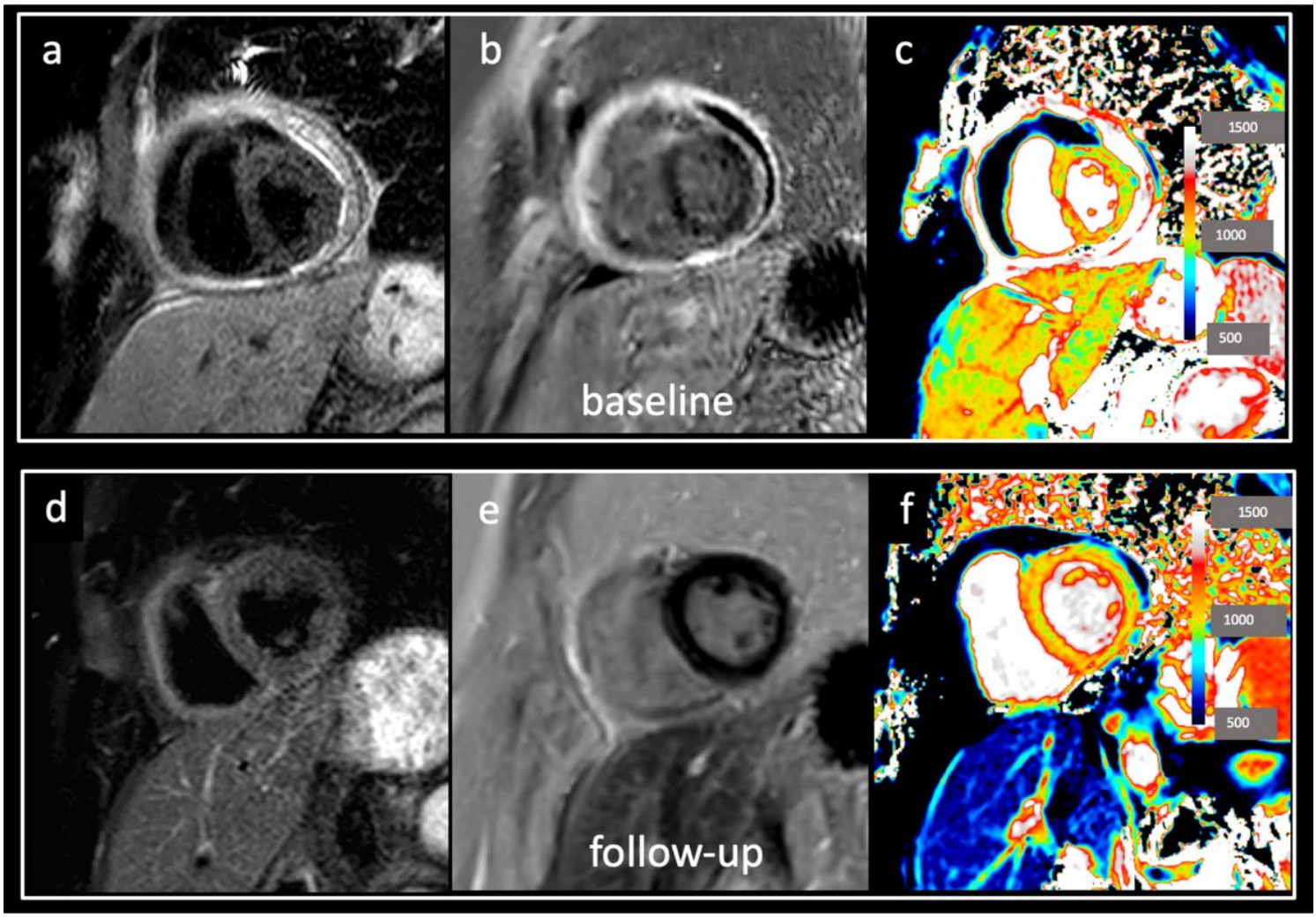

Figure 5

Inflammatory-effusive pericarditis with constrictive physiology. 49-year-old woman with bacterial pericarditis presenting with malaise, NYHA 2, fever and pitting edema in lower limbs. CRP 84 mg/L. Increased liver enzymes (GGT 254 U/L). CMR performed after pericardiocentesis showed edematous thickened pericardial layers (panel a) with strong enhancement (panel b) and mild residual effusion (panel b). Strongly increased T1 liver values (>1000 ms). Free breathing cine MR imaging (video 2a) showed inspiratory diastolic septal inversion with increased respiratory septal shift (36%). Follow-up

cardiovascular MR imaging 4 months after optimized medical therapy showed disappearance of pericardial edema with near normalization of pericardial thickness (panel d), minimal residual pericardial enhancement (panel e), and a normalization of T1 liver values (620 ms)(panel f). Normalization of ventricular coupling (video 2b).

Supplementary Files

This is a list of supplementary files associated with this preprint. Click to download.

- SupplementaryFig1.tif
- SupplementaryFig2.tif
- video1a.mov
- video1b.mov
- video1c.mov
- video1d.mov
- video2a.mov
- video2b.mov
- SupplFileSection.docx